


Article

Characterization of GAGG Doped with Extremely Low Levels of Chromium and Exhibiting Exceptional Intensity of Emission in NIR Region

Greta Inkrataite ^{1,*} , Gerardas Laurinavicius ¹, David Enseling ², Aleksej Zarkov ¹ , Thomas Jüstel ²  and Ramunas Skaudzius ¹

¹ Faculty of Chemistry and Geosciences, Institute of Chemistry, Vilnius University, Naugarduko 24, LT-03225 Vilnius, Lithuania; gerardas.laurinavicius@chgf.stud.vu.lt (G.L.); aleksej.zarkov@chf.vu.lt (A.Z.); ramunas.skaudzius@chgf.vu.lt (R.S.)

² Department of Chemical Engineering, Münster University of Applied Sciences, Stegerwaldstrasse 39, D-48565 Steinfurt, Germany; david.enseling@fh-muenster.de (D.E.); tj@fh-muenster.de (T.J.)

* Correspondence: greta.inkrataite@chgf.vu.lt; Tel.: +370-5-219-3105

Abstract: Cerium and chromium co-doped gadolinium aluminum gallium garnets were prepared using sol-gel technique. These compounds potentially can be applied for NIR-LED construction, horticulture and theranostics. Additionally, magnesium and calcium ions were also incorporated into the structure. X-ray diffraction data analysis confirmed the all-cubic symmetry with an Ia-3d space group, which is appropriate for garnet-type materials. From the characterization of the luminescence properties, it was confirmed that both chromium and cerium emissions could be incorporated. Cerium luminescence was detected under 450 nm excitation, while for chromium emission, 270 nm excitation was used. The emission of chromium ions was exceptionally intense, although it was determined that these compounds are doped only by parts per million of Cr³⁺ ions. Typically, the emission maxima of chromium ions are located around 650–750 nm in garnet systems. However, in this case, the emission maximum for chromium is measured to be around 790 nm, caused by re-absorption of Cr³⁺ ions. The main observation of this study is that the switchable emission wavelength in a compound of single phase was obtained, despite the fact that doping with Cr ions was performed in ppm level, causing an intense emission in NIR region.

Keywords: cerium; chromium; garnets; luminescence; NIR; sol-gel synthesis



Citation: Inkrataite, G.; Laurinavicius, G.; Enseling, D.; Zarkov, A.; Jüstel, T.; Skaudzius, R. Characterization of GAGG Doped with Extremely Low Levels of Chromium and Exhibiting Exceptional Intensity of Emission in NIR Region. *Crystals* **2021**, *11*, 673. <https://doi.org/10.3390/cryst11060673>

Academic Editor:
Alessandro Chiasera

Received: 27 May 2021
Accepted: 9 June 2021
Published: 11 June 2021

Publisher's Note: MDPI stays neutral with regard to jurisdictional claims in published maps and institutional affiliations.



Copyright: © 2021 by the authors. Licensee MDPI, Basel, Switzerland. This article is an open access article distributed under the terms and conditions of the Creative Commons Attribution (CC BY) license (<https://creativecommons.org/licenses/by/4.0/>).

1. Introduction

In recent years, more and more scientists have focused on the synthesis and development of functional inorganic materials. Two of the main considered groups of such compounds are the inorganic scintillators and phosphors. Inorganic scintillators are widely used in medicine and nuclear physics as the x-ray converter material for CT and others detectors [1–4], while inorganic phosphors are mainly used as material in light-emitting diodes (LEDs) [5–7].

Scintillator and phosphor materials usually consist of a host matrix and activator ions, which, in most cases, are lanthanide or transition metal ions [8]. While the host and activator strategy is the most common, there are other types of materials which possess intrinsic luminescence as well [9,10]. However, lanthanum, promethium, and lutetium are not suitable for such applications. One of the most popular groups of host materials are garnets, which are oxides crystallizing in a cubic structure with space group Ia3d, and which comprise three differently coordinated cation sites, namely dodecahedral, octahedral, and tetrahedral positions [11,12]. The host material used in this study was gadolinium aluminum gallium garnet (GAGG), with the formula Gd₃Al₂Ga₃O₁₂. GAGG:Ce garnets exhibited the brightest light yields of 46,000 ph/MeV among other oxide crystalline scintillators [13,14]. Despite the fact that there is a wide variety of dopant ions used in scintillator

production, GAGG is mostly doped just by Ce^{3+} ions [15–18]. There has been a number of studies in recent years about various GAGG:Ce modifications and the resulting changes in luminescence properties. It has been shown that by changing the ratio between Al and Ga in the garnet structure, Ce emission band can be shifted due to the change of crystal field splitting. It is worthy to note that such changes in emission maxima are also present in other garnets doped with cerium ions, such as $\text{Lu}_3\text{Al}_5\text{O}_{12}:\text{Ce}$ (LuAG:Ce) or $\text{Y}_3\text{Al}_5\text{O}_{12}:\text{Ce}$ (YAG:Ce) [11,19–21]. Another type of modification for GAGG:Ce is co-doping with various metal cations. Studies have shown that co-doping of GAGG:Ce with mono/di/trivalent cations usually affects the luminescence, i.e., the absorption strength, quantum efficiency, quenching temperature, and decay time [17,22–31]. The change of these parameters depends not only on the dopant type, but also on its concentration. These changes are thought to be caused by the formation of various localized energy levels in the conduction band of the garnet, due to the crystal defects which are formed when Gd^{3+} ions are replaced with cations of different valence c(1+, 2+ or sometimes 4+) [11].

The impact of Cr^{3+} on Ce^{3+} decay time was observed in YAG:Ce,Cr. In this case, the decay time greatly increased with the introduction of high amount (500 ppm) of chromium ions [32]. It was proposed that Cr^{3+} co-doping results in the formation of electron trapping sites with an ideal trap depth for persistent luminescence at room temperature [28,32]. It was also proposed and proven that the same principles can be applied to the GAGG phosphor luminescence where co-doping of Cr^{3+} and Ce^{3+} results in persistent phosphor luminescence of excited Ce^{3+} sites and, in some cases, Cr^{3+} emission in the visible range [28–30,32,33]. In this study, a novel system consisting of GAGG matrix and four additional dopant elements (Ce^{3+} , Cr^{3+} , Mg^{2+} and Ca^{2+}) was investigated. Since the chromium concentration is just in the ppm range, it exhibits not typical chromium emission but the maximum of emission band is shifted towards 790 nm. Such emission in the near infrared region (NIR) range might be useful for plant growth purposes [34]. Additionally, these compounds could be used in the fabrication of high power NIR-LED devices for night vision applications, and biosensors used to measure content of water, fat, sugar, protein of different products [35,36]. Therefore, in turn, these phosphors could be potentially applied in horticulture research experiments. Biological tissue transmits radiation in the range from 650 to 1300 nm (the first biological window), which allows deeper penetration, so such compounds could also be promising candidates in the field of theranostics [37,38].

2. Materials and Methods

Gadolinium aluminum gallium garnet powders were synthesized by the sol-gel method. Cerium concentration was kept at 0.05 mol% for all samples. All synthesized powder compounds are listed in Table 1.

Table 1. Chemical composition of synthesized powders determined by ICP-OES.

Name of Sample	Formula of Sample
Sample 1	GAGG: Ce 0.05%, Ca 100 ppm, Mg 7 ppm, Cr 15 ppm
Sample 2	GAGG: Ce 0.05%, Ca 94 ppm, Mg 8 ppm, Cr 15 ppm
Sample 3	GAGG: Ce 0.05%, Ca 57 ppm, Mg 9 ppm, Cr 15 ppm

For these compounds, Gd_2O_3 , Ga_2O_3 , $\text{Al}(\text{NO}_3)_3 \cdot 9\text{H}_2\text{O}$, $(\text{NH}_4)_2\text{Ce}(\text{NO}_3)_6$, $\text{Ca}(\text{NO}_3)_2 \cdot 4\text{H}_2\text{O}$ and $\text{Mg}(\text{NO}_3)_2 \cdot 6\text{H}_2\text{O}$ were used as precursors. Firstly, Gd_2O_3 and Ga_2O_3 were dissolved in an excess of concentrated nitric acid at 50 °C. Then, the acid was evaporated and the remaining gel was washed with distilled water 2 or 3 times, followed by further evaporation of added water. An additional 200 mL of water was added after the washing, and $\text{Al}(\text{NO}_3)_3 \cdot 9\text{H}_2\text{O}$, $(\text{NH}_4)_2\text{Ce}(\text{NO}_3)_6$, $\text{Ca}(\text{NO}_3)_2 \cdot 9\text{H}_2\text{O}$ and $\text{Mg}(\text{NO}_3)_2 \cdot 9\text{H}_2\text{O}$ were dissolved. The solution was left under magnetic stirring for 2 h at 50–60 °C. After that, citric acid was added to the solution with a ratio of 3:1 to metal ions, and was left to stir overnight. The solution was evaporated at the same temperature, and the obtained gels were dried at 140 °C for 24 h in the oven. The obtained powders were ground and annealed first at

1000 °C for 2 h in air, with 5 °C/min heating rate. Secondly, the gained powders were heated at 1400 °C for 4 h, with 5 °C/min heating rate.

X-ray diffraction (XRD) measurements of the powders were performed using the Rigaku MiniFlex II X-ray diffractometer (Rigaku Europe SE, Neu-Isenburg, Germany). Powders used for analysis were evenly dispersed on the glass sample holder using ethanol. Then diffraction patterns were recorded in the range of 2θ angles from 15° to 80° for all compounds. Cu K_{α} radiation ($\lambda = 1.542 \text{ \AA}$ (Average of Cu $K_{\alpha 1} = 1.540$ and $K_{\alpha 2} = 1.544$)) was used for the analysis. The measurement parameters were set as follows: current was 15 mA, voltage –30 kV, X-ray detector movement step was 0.010° and dwell time was 5.0 s.

Measurements of emission and excitation: Edinburgh Instruments FLS980 spectrometer (Edinburgh Instruments, Livingston, UK) equipped with double excitation and emission monochromators and 450 W Xe arc lamp (Edinburgh Instruments, Livingston, UK) a cooled (–20 °C) single-photon counting photomultiplier (Hamamatsu R928(Edinburgh Instruments, Livingston, UK)) and mirror optics for powder samples were used for measuring the excitation and emission of the prepared samples. Obtained photoluminescence emission spectra were corrected using a correction file obtained from a tungsten incandescent lamp certified by National Physics Laboratory (NPL), UK. Excitation spectra were corrected by a reference detector [39]. The reflectance spectra from 250 to 600 nm were measured in an integrated (solid) sphere coated with barium sulphate. BaSO₄ (99% Sigma-Aldrich, St. Louis, Missouri, United States) was used as a reference material, with excitation and emission gaps of 4 and 0.15 nm, respectively. Each measurement was performed 10 times. Measurements in the range of 120 to 400 nm were performed using a FLS920 fluorescence spectrometer (Edinburgh Instruments, Livingston, UK) with an R-UV excitation monochromator VM504 (Acton Research Corporation, Acton, Massachusetts, USA) and a deuterium lamp (Edinburgh Instruments, Livingston, UK) in a BAM:Eu (BaMgAl₁₀O₁₇:Eu²⁺)-coated integrated sphere. The measuring chamber containing the sample was continuously flushed with dry nitrogen gas to remove water and oxygen, since these molecules show vacuum UV absorption. The photoluminescence decay kinetics were studied for powders and thin films using the FLS980 spectrometer(Edinburgh Instruments, Livingston, UK). 450 nm lasers were used for these measurements [39].

Identification of quantification of Ca, Mg, and Cr in the synthesized species was performed by inductively coupled plasma optical emission spectrometry (ICP-OES) using Perkin-Elmer Optima 7000 DV spectrometer (Perkin-Elmer, Waltham, MA, USA). Sample decomposition procedure was carried out in concentrated nitric acid (HNO₃, Rotipuran® Supra 69% (Roth, Karlsruhe, Germany)) using microwave reaction system Anton Paar Multiwave 3000 (Anton-Paar, Graz, Austria) equipped with XF100 rotor and PTFE liners (Anton-Paar, Graz, Austria). The following program was used for the dissolution of powders: during the first step, the microwave power was linearly increased to 800 W in 15 min and held at this point for the next 20 min. Once the vessels had been fully cooled and depressurized, the obtained clear solutions were quantitatively transferred into volumetric flasks and diluted up to 50 mL with deionized water. Calibration solutions were prepared by an appropriate dilution of the stock standard solutions (single-element ICP standards, 1000 mg/L, (Roth, Karlsruhe, Germany)).

3. Results and Discussion

3.1. X-ray Diffraction Analysis

To determine the phase purity of the powder garnet samples, XRD analysis was performed. Figure 1 shows the diffraction patterns of all synthesized garnets. From the displayed data, it can be concluded that all compounds, regardless of the concentrations of doping elements, possess cubic GAGG structure with Ia-3d space group ((PDF) #00-046-0448). No peaks corresponding to the constituent oxides were observed. However, we can observe a slight shift of the peaks from the PDF card data to smaller 2θ angles. This shift was due to additional doping of the compound with Mg²⁺, Ca²⁺, Ce³⁺, and/or Cr³⁺ ions, due to the ionic radii difference [40]. In summary, from the measured data,

it can be concluded that garnets could be doped without the formation of additional impurity phases.

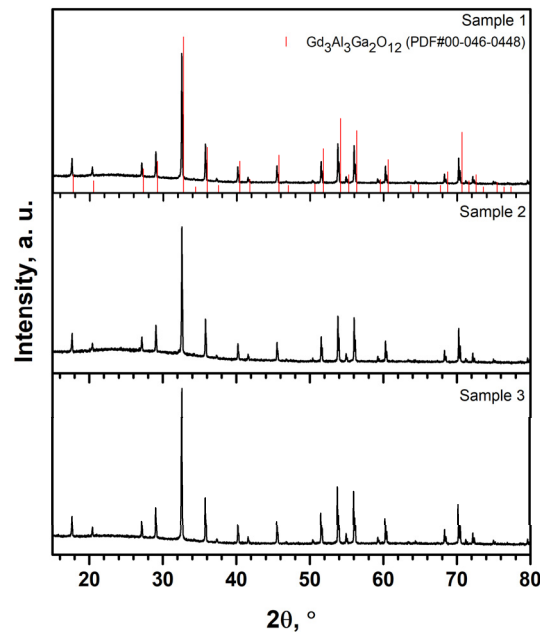


Figure 1. XRD patterns of the GAGG:Ce,Cr,Mg,Ca micropowder samples.

3.2. Luminescence Properties

For the practical application of luminescent materials, they have to emit a rather discreet wavelength light, due to the fact that light interacts differently based on its wavelength. Photons with NIR wavelengths are especially important, and they have deeper tissue penetration and can induce faster plant growth. Additionally, should the possibly arise to switch between NIR and other wavelengths in a single matrix, a new application area could potentially be available. In this case, the luminescence is induced by exciting one of the trivalent ions used as dopants (Ce^{3+} , Cr^{3+}). Upon recording the emission and excitation of the compounds, electronic transitions of both cerium and chromium ions can be observed. The absorption bands that are ascribed to cerium ions are due to inter-configurational $[\text{Xe}]4f^1-[\text{Xe}]5d^1$ transitions, while in the case of Cr^{3+} intraconfigurational $[\text{Ar}]3d^3-[\text{A}]3d^3$ transitions between the crystal-field components, $^4\text{A}_1$ and $^4\text{T}_1$ are observed. Due to the allowed nature of these electron transitions, broad emission bands are detected. During these processes, energy is either reemitted or just absorbed, which defines the optical properties of such garnets. Given the possibility to switch between cerium and chromium emission based on the excitation wavelength, as well as the large red shift of chromium emission toward 790 nm, such compounds could potentially be good candidates as multifunctional materials in horticultural and theranostic applications. However, further research for practical applications is still needed to evaluate such possibilities more in-depth.

In order to estimate optical properties of the synthesized materials excitation, emission and reflectance spectra were recorded. The decay times were measured as well. Figures 2 and 3 show the excitation and emission spectra of different GAGG compounds measured at room temperature. In Figure 2, the recorded chromium emission and excitation spectra are displayed. In excitation spectra, the most intense band is attributed to $^8\text{S}_{7/2}-^6\text{I}_j$ transitions of Gd^{3+} ions with the maxima at 270 nm. At 415 and 575 nm, the evidence of excitation process of chromium ions resulting from the transitions between $^4\text{A}_1$ to $^4\text{T}_1$ and $^4\text{T}_2$ orbitals was also observed. Meanwhile, the emission signal detected under 270 nm excitation is caused by the transition from $^4\text{T}_2$ to $^4\text{A}_1$ orbital. From the spectra given in Figure 2, it can be derived that the compound with the highest content of magnesium

(Sample 3), i.e., 9 ppm, exhibits the most intense emission and excitation bands. The difference in the intensity of excitation and emission could be attributed to the different calcium content in the compounds. Since calcium has a 2+ charge and it is introduced instead of 3+ gadolinium ion, oxygen vacancy defects are most likely created, due to the aliovalent nature of substitution. It is commonly known that such defects reduce the luminescence intensity of most compounds [41,42]. In this case, the compound with the lowest Ca^{2+} amount (Sample 3) has the highest luminescence intensity, whereas Sample 1 and Sample 2 have similar amounts Ca^{2+} ions and show lower emission intensities. It should be noted that chromium is present in ppm fractions, nevertheless, its emission remains very intense. Commonly, chromium emission maximum in garnet matrix is around 650–750 nm, while in this case it was measured to be 790 nm. Such a shift to the red region was previously explained by the re-absorption of Cr^{3+} ions [43]. Studies by other researchers revealed that a high photoluminescence intensity of chromium ions emission was only recorded with 2000 times higher amounts (for example, 3 mol%) of Cr^{3+} in other compounds [44].

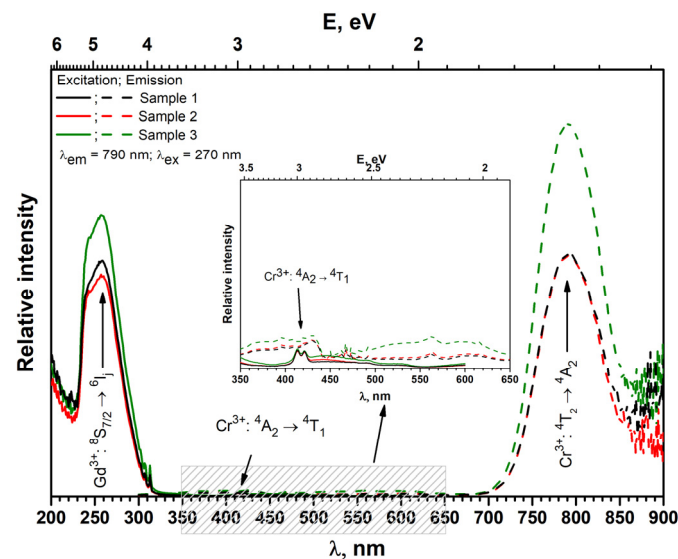


Figure 2. Excitation and emission spectra of GAGG:Ce,Cr,Mg,Ca powder samples ($\lambda_{\text{ex}} = 270$ nm). Inset represents zoomed in spectral region from 350 to 650 nm.

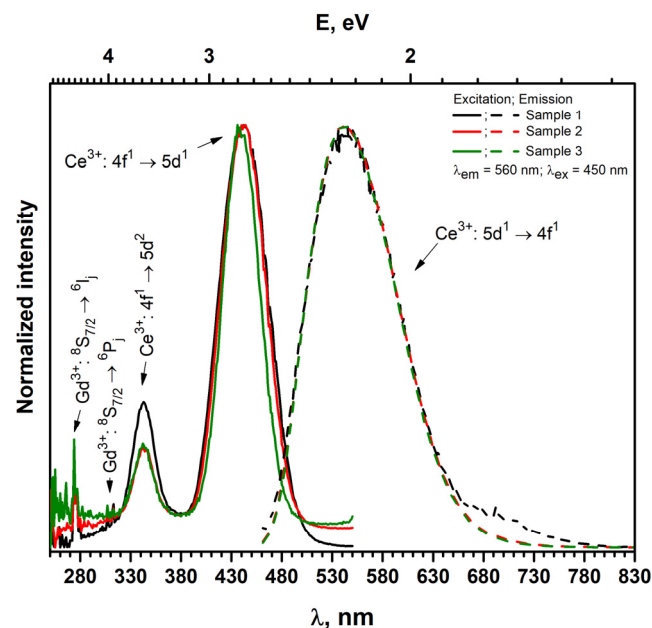


Figure 3. Excitation and emission spectra of GAGG:Ce,Cr,Mg,Ca powder samples ($\lambda_{\text{ex}} = 450$ nm).

Since these garnets were doped with cerium as well, they also have the characteristic emission attributed to cerium ions. Normalized emission is attributed to cerium emission, and excitation spectra are shown in Figure 3. To measure cerium emission, the compounds were excited under 450 nm wavelength ($[\text{Xe}]4f^1$ to $[\text{Xe}]5d^1$ interconfigurational transitions of Ce^{3+}), which cannot be attributed to chromium. The compounds appear to exhibit cerium-specific fluorescence at a wavelength of 540 nm, which arises from the $5d^1$ to $4f^1$ electronic transitions. Meanwhile, when investigating the excitation spectra of the compounds in addition to those cerium bands, the peaks contributing to gadolinium ions were observed in the 250–320 nm range [19,44].

Figure 4 shows the reflectance spectra of the compounds. In the reflectance spectra of garnets doped with cerium, two absorption bands can be observed, one at about 350 nm, the another at 400–500 nm. These bands are assigned to the different crystal-field components of the interconfigurational $\text{Ce}^{3+} [\text{Xe}]4f^1 \rightarrow [\text{Xe}]5d^1$ transitions. At approximately 275 nm, an absorption peak is observed in all spectra, which is assigned to the $\text{Gd}^{3+} {}^8S_{7/2} \rightarrow {}^6I_J$ interconfigurational transitions. The set of absorption peaks at about 312 nm is assigned to the $\text{Gd}^{3+} {}^8S_{7/2} \rightarrow {}^6P_J$ electron transitions [19,45]. It should be noted that the position of the Ce^{3+} absorption bands does not change upon changing the ions with which the garnet was doped, so it could be stated that doping with magnesium and calcium does not affect the absorption wavelength. However, it is obvious that garnets also have cerium. The absorption band at 360 and 440 nm is classified as a Ce^{3+} electronic transition. In addition, there is no bright absorption band at 600 nm, which is typically observed in Cr^{3+} -containing compounds [44,46–48].

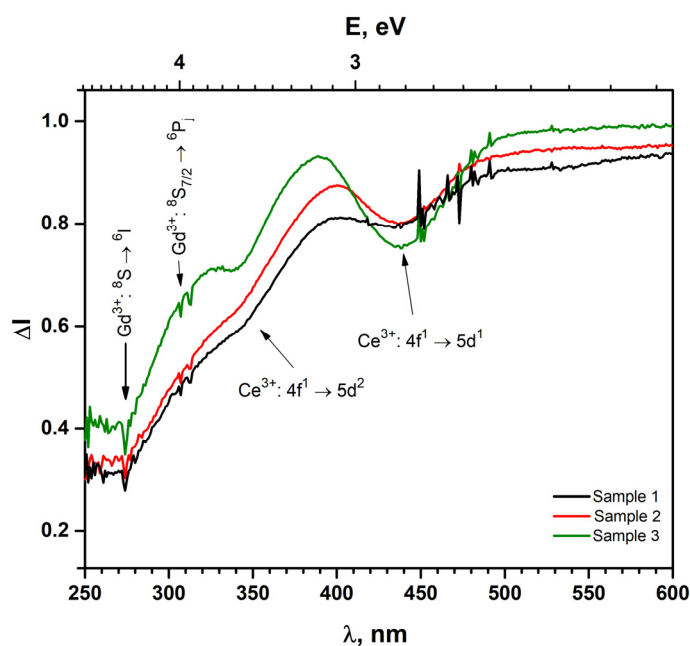


Figure 4. Diffuse reflection spectra of GAGG:Ce,Cr,Mg,Ca powder samples.

To better investigate the absorption of garnets in the UV region, the reflectance spectra of the synthesized gadolinium aluminum gallium garnets powders in the 130–400 nm range were recorded. The reflectance spectra are shown in Figure 5. It can be seen that in the 130–400 nm region, three clear absorption bands are visible: one in the 140–165 nm range, the second in the 190–240 nm range, and the last in 270–280 nm zone. The absorption in the 270–280 nm range can be attributed to $\text{Gd}^{3+} {}^8S \rightarrow {}^6I$ electron transitions [19]. The observed absorption in the 140–165 nm range can be interpreted as the electron jump into the Ce^{3+} 5d orbital [49,50]. Finally, the region of 200–300 nm can be explained as the band gap absorption of the garnet matrix [50,51].

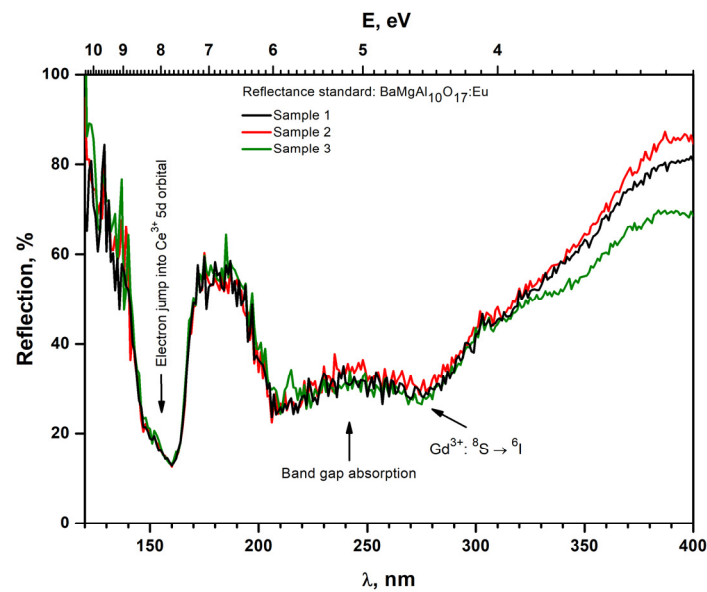


Figure 5. Reflection spectra of GAGG:Ce,Cr,Mg,Ca powder samples in the UV region.

The photoluminescence decay curves of the chromium emission are shown in Figure 6. All calculated values of the decay times are listed in Table 2. As can be seen from Table 2, all compounds have almost the same decay times, which are between 6.0 and 5.9 ms. It can be seen that the samples have emission decay times showing the characteristics of Cr^{3+} ions, because characteristic decay times for Ce^{3+} ions are much shorter and reach about 50–60 ns [5,52]. Cr^{3+} ions electron transition are considered forbidden, which usually results in longer decay times in a range of milliseconds [42,53]. However, for the Ce^{3+} ions, electron transitions are allowed, and the decay time is in the range of nanoseconds [5]. The obtained values are of chromium, since the 270 nm excitation wavelength was used. While there have been previous reports on the effect of calcium and magnesium doping in garnet matrix on decay times [17,54–56], in this case, no effect was observed, potentially due to the drastically smaller amounts to aforementioned ions.

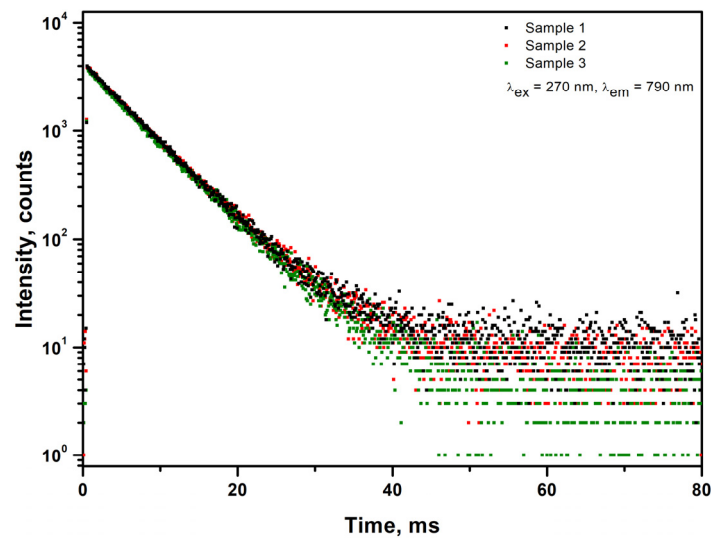


Figure 6. Decay curves of the Cr^{3+} emission of the GAGG:Ce,Cr,Mg,Ca powder samples upon 270 nm excitation.

Table 2. Synthesized powder samples.

Sample	Decay Time (ms)
GAGG: Ce 0.05%, Ca 100 ppm, Mg 7 ppm, Cr 15 ppm (Sample 1)	5.9
GAGG: Ce 0.05%, Ca 94 ppm, Mg 8 ppm, Cr 15 ppm (Sample 2)	6
GAGG: Ce 0.05%, Ca 57 ppm, Mg 9 ppm, Cr 15 ppm (Sample 3)	6

4. Conclusions

Gadolinium aluminum gallium garnets doped with 0.05% cerium, chromium, magnesium, and calcium were synthesized by the sol-gel method whereby obtained garnet type samples are of single phase. Measurement of the excitation and emission spectra of these compounds revealed that extremely low levels of Cr^{3+} ions, i.e., only at a level of 15 ppm, caused intense emission in the NIR region. At the same time, but under different excitation wavelengths, a typical emission spectrum of Ce^{3+} was also observed, which proved that the single compound might emit in very broad range (from 470 to 850 nm). The most intense emission was located at a wavelength of 790 nm. The obtained compounds exhibit promising luminescence properties to illuminate plants and promote their growth. Since luminescence covered the first biological window and chromium ions exhibited a long specific decay time in the range of 6 ms, the synthesized compounds also demonstrate characteristics required for bio-imaging purposes.

Author Contributions: R.S. and G.I. conceived and planned the experiments and wrote the manuscript with support from other co-authors, G.L. and G.I. synthesized powders, R.S. supervised the project, A.Z. performed ICP measurements of powders, G.L. performed XRD measurements, D.E., G.L. and T.J. performed luminescence measurements, and T.J. analyzed luminescence properties. All authors provided critical feedback and helped shape the research, analysis and manuscript. All authors have read and agreed to the published version of the manuscript.

Funding: This research received no external funding.

Institutional Review Board Statement: Not applicable.

Informed Consent Statement: Not applicable.

Conflicts of Interest: The authors declare no conflict of interest.

References

- Paper, C.; Cherepy, N.; Livermore, L.; Seeley, Z.M.; Livermore, L.; Beck, P.; Livermore, L.; Hunter, S.L.; Livermore, L. High Energy Resolution Transparent Ceramic Garnet Scintillators. *Int. Soc. Opt. Photonics* **2014**, *2*. [[CrossRef](#)]
- Sakthong, O.; Chewpraditkul, W.; Wanarak, C.; Kamada, K. Nuclear Instruments and Methods in Physics Research A Scintillation Properties of $\text{Gd}_3\text{Al}_2\text{Ga}_3\text{O}_{12}:\text{Ce}_3\text{p}$ Single Crystal Scintillators. *Nucl. Inst. Methods Phys. Res. A* **2014**, *751*, 1–5. [[CrossRef](#)]
- Belli, P.; Bernabei, R.; Cerulli, R.; Dai, C.J.; Danevich, F.A.; Incicchitti, A.; Kobychyev, V.V.; Ponkratenko, O.A.; Prosperi, D.; Tretyak, V.I.; et al. Performances of a CeF_3 Crystal Scintillator and Its Application to the Search for Rare Processes. *Nucl. Instrum. Methods Phys. Res. Sect. A Accel. Spectrometers Detect. Assoc. Equip.* **2003**, *498*, 352–361. [[CrossRef](#)]
- Van Eijk, C.W.E. *Scintillator-Based Detectors*; Elsevier B.V.: Amsterdam, The Netherlands, 2014; Volume 8. [[CrossRef](#)]
- Bachmann, V.; Ronda, C.; Meijerink, A. Temperature Quenching of Yellow Ce^{3+} Luminescence in $\text{YAG}:\text{Ce}$. *Chem. Mater.* **2009**, *21*, 2077–2084. [[CrossRef](#)]
- Khaidukov, N.; Zorenko, T.; Iskaliyeva, A.; Paprocki, K.; Batentschuk, M.; Osvet, A.; Van Deun, R.; Zhydaczevskii, Y.; Suchocki, A.; Zorenko, Y. Synthesis and Luminescent Properties of Prospective Ce^{3+} Doped Silicate Garnet Phosphors for White LED Converters. *J. Lumin.* **2017**, *192*, 328–336. [[CrossRef](#)]
- Ueda, J.; Dorenbos, P.; Bos, A.J.J.; Meijerink, A.; Tanabe, S. Insight into the Thermal Quenching Mechanism for $\text{Y}_3\text{Al}_5\text{O}_{12}:\text{Ce}^{3+}$ through Thermoluminescence Excitation Spectroscopy. *J. Phys. Chem. C* **2015**, *119*, 25003–25008. [[CrossRef](#)]
- Auffray, E.; Korjik, M.; Lucchini, M.T.; Nargelas, S.; Sidletskiy, O.; Tamulaitis, G.; Tratsiak, Y.; Vaitkevicius, A. Free Carrier Absorption in Self-Activated PbWO_4 and Ce-Doped $\text{Y}_3(\text{Al}_{0.25}\text{Ga}_{0.75})_3\text{O}_{12}$ and $\text{Gd}_3\text{Al}_2\text{Ga}_3\text{O}_{12}$ Garnet Scintillators. *Opt. Mater.* **2016**, *58*, 461–465. [[CrossRef](#)]
- Seminko, V.; Maksimchuk, P.; Bespalova, I.; Masalov, A.; Viagin, O.; Okrushko, E.; Kononets, N.; Malyukin, Y. Defect and Intrinsic Luminescence of CeO_2 Nanocrystals. *Phys. Status Solidi* **2017**, *254*, 1600488. [[CrossRef](#)]

10. Zatsepin, D.A.; Boukhvalov, D.W.; Zatsepin, A.F.; Kuznetsova, Y.A.; Mashkovtsev, M.A.; Rychkov, V.N.; Shur, V.Y.; Esin, A.A.; Kurmaev, E.Z. Electronic Structure, Charge Transfer, and Intrinsic Luminescence of Gadolinium Oxide Nanoparticles: Experiment and Theory. *Appl. Surf. Sci.* **2018**, *436*, 697–707. [[CrossRef](#)]
11. Kanai, T.; Satoh, M.; Miura, I. Characteristics of a Nonstoichiometric $Gd^{3+\delta}(Al,Ga)_{5-\Delta}O_{12}:Ce$ Garnet Scintillator. *J. Am. Ceram. Soc.* **2008**, *91*, 456–462. [[CrossRef](#)]
12. Geller, S. Magnetic Interactions and Distribution of Ions in the Garnets. *J. Appl. Phys.* **1960**, *30*. [[CrossRef](#)]
13. Yanagida, T.; Kamada, K.; Fujimoto, Y.; Yagi, H.; Yanagitani, T. Comparative Study of Ceramic and Single Crystal Ce:GAGG Scintillator. *Opt. Mater.* **2013**, *35*, 2480–2485. [[CrossRef](#)]
14. Fedorov, A.; Gurinovich, V.; Guzov, V.; Dosovitskiy, G.; Korzhik, M.; Kozhemyakin, V.; Lopatik, A.; Kozlov, D.; Mechinsky, V.; Retivov, V. Sensitivity of GAGG Based Scintillation Neutron Detector with SiPM Readout. *Nucl. Eng. Technol.* **2020**, *52*, 2306–2312. [[CrossRef](#)]
15. Kitaura, M.; Sato, A.; Kamada, K.; Kurosawa, S.; Ohnishi, A.; Sasaki, M.; Hara, K. Photoluminescence Studies on Energy Transfer Processes In. *Opt. Mater.* **2015**, *41*, 45–48. [[CrossRef](#)]
16. Kitaura, M.; Sato, A.; Kamada, K.; Ohnishi, A.; Sasaki, M. Phosphorescence of Ce-Doped $Gd_3Al_2Ga_3O_{12}$ Crystals Studied Using Luminescence Spectroscopy. *J. Appl. Phys.* **2014**, *115*, 10–18. [[CrossRef](#)]
17. Lucchini, M.T.; Gundacker, S.; Lecoq, P.; Benaglia, A.; Nikl, M.; Kamada, K.; Yoshikawa, A.; Auffray, E. Timing Capabilities of Garnet Crystals for Detection of High Energy Charged Particles. *Nucl. Instruments Methods Phys. Res. Sect. A Accel. Spectrometers Detect. Assoc. Equip.* **2017**, *852*, 1–9. [[CrossRef](#)]
18. Gundacker, S.; Turtos, R.M.; Auffray, E.; Lecoq, P. Precise Rise and Decay Time Measurements of Inorganic Scintillators by Means of X-Ray and 511 KeV Excitation. *Nucl. Instrum. Methods Phys. Res. Sect. A Accel. Spectrometers Detect. Assoc. Equip.* **2018**, *891*, 42–52. [[CrossRef](#)]
19. Ogieg, J.M.; Katelnikovas, A.; Zych, A.; Ju, T.; Meijerink, A.; Ronda, C.R. Luminescence and Luminescence Quenching in $Gd_3(Ga,Al)_5O_{12}$ Scintillators Doped with Ce^{3+} . *J. Phys. Chem. A* **2013**, *117*, 2479–2484. [[CrossRef](#)] [[PubMed](#)]
20. Ueda, J.; Tanabe, S.; Nakanishi, T. Analysis of Ce^{3+} Luminescence Quenching in Solid Solutions between $Y_3Al_5O_{12}$ and $Y_3Ga_5O_{12}$ by Temperature Dependence of Photoconductivity Measurement. *J. Appl. Phys.* **2011**, *110*, 053102. [[CrossRef](#)]
21. Pan, Y.; Wu, M.; Su, Q. Tailored Photoluminescence of YAG:Ce Phosphor through Various Methods. *J. Phys. Chem. Solids* **2004**, *65*, 845–850. [[CrossRef](#)]
22. Yoshino, M.; Kamada, K.; Kochurikhin, V.V.; Ivanov, M.; Nikl, M.; Okumura, S.; Yamamoto, S.; Yeom, J.Y.; Shoji, Y.; Kurosawa, S.; et al. Li^+ , Na^+ and K^+ Co-Doping Effects on Scintillation Properties of Ce: $Gd_3Ga_3Al_2O_{12}$ Single Crystals. *J. Cryst. Growth* **2018**, *491*, 1–5. [[CrossRef](#)]
23. Kobayashi, T.; Yamamoto, S.; Yeom, J.; Kamada, K.; Yoshikawa, A. Development of High Resolution Phoswich Depth-of-Interaction Block Detectors Utilizing Mg Co-Doped New Scintillators. *Nucl. Inst. Methods Phys. Res. A* **2017**. [[CrossRef](#)]
24. Meng, F.; Koschan, M.; Wu, Y.; Melcher, C.L. Relationship between Ca^{2+} Concentration and the Properties of Codoped $Gd_3Ga_3Al_2O_{12}:Ce$ Scintillators. *Nucl. Instrum. Methods Phys. Res. Sect. A Accel. Spectrometers Detect. Assoc. Equip.* **2015**, *797*, 138–143. [[CrossRef](#)]
25. Kamada, K.; Shoji, Y.; Kochurikhin, V.V.; Nagura, A.; Okumura, S.; Yamamoto, S.; Yeom, J.Y.; Kurosawa, S.; Pejchal, J.; Yokota, Y.; et al. Single Crystal Growth of Ce: $Gd_3(Ga,Al)_5O_{12}$ with Various Mg Concentration and Their Scintillation Properties. *J. Cryst. Growth* **2017**, *468*, 407–410. [[CrossRef](#)]
26. Lucchini, M.T.; Babin, V.; Bohacek, P.; Gundacker, S.; Kamada, K.; Nikl, M.; Petrosyan, A.; Yoshikawa, A.; Auffray, E. Effect of Mg^{2+} Ions Co-Doping on Timing Performance and Radiation Tolerance of Cerium Doped $Gd_3Al_2Ga_3O_{12}$ Crystals. *Nucl. Instrum. Methods Phys. Res. Sect. A Accel. Spectrometers Detect. Assoc. Equip.* **2016**, *816*, 176–183. [[CrossRef](#)]
27. Auffray, E.; Augulis, R.; Fedorov, A.; Dosovitskiy, G.; Grigorjeva, L.; Gulbinas, V.; Koschan, M.; Lucchini, M.; Melcher, C.; Nargelas, S.; et al. Excitation Transfer Engineering in Ce-Doped Oxide Crystalline Scintillators by Codoping with Alkali-Earth Ions. *Phys. Status Solidi Appl. Mater. Sci.* **2018**, *215*, 1–10. [[CrossRef](#)]
28. Ueda, J.; Kuroishi, K.; Tanabe, S. Yellow Persistent Luminescence in $Ce^{3+}-Cr^{3+}$ -Codoped Gadolinium Aluminum Gallium Garnet Transparent Ceramics after Blue-Light Excitation. *Appl. Phys. Express* **2014**, *7*. [[CrossRef](#)]
29. Asami, K.; Ueda, J.; Tanabe, S. Trap Depth and Color Variation of $Ce^{3+}-Cr^{3+}$ Co-Doped $Gd_3(Al,Ga)_5O_{12}$ Garnet Persistent Phosphors. *Opt. Mater.* **2016**, *62*, 171–175. [[CrossRef](#)]
30. Gotoh, T.; Jeem, M.; Zhang, L.; Okinaka, N.; Watanabe, S. Synthesis of Yellow Persistent Phosphor Garnet by Mixed Fuel Solution Combustion Synthesis and Its Characteristic. *J. Phys. Chem. Solids* **2020**, *142*, 109436. [[CrossRef](#)]
31. Tamulaitis, G.; Vaitkevičius, A.; Nargelas, S.; Augulis, R.; Gulbinas, V.; Bohacek, P.; Nikl, M.; Borisevich, A.; Fedorov, A.; Korjik, M.; et al. Subpicosecond Luminescence Rise Time in Magnesium Codoped GAGG:Ce Scintillator. *Nucl. Instruments Methods Phys. Res. Sect. A Accel. Spectrometers Detect. Assoc. Equip.* **2017**, *870*, 25–29. [[CrossRef](#)]
32. Ueda, J.; Kuroishi, K.; Tanabe, S. Bright Persistent Ceramic Phosphors of $Ce^{3+}-Cr^{3+}$ -Codoped Garnet Able to Store by Blue Light. *Appl. Phys. Lett.* **2014**, *104*, 5–9. [[CrossRef](#)]
33. Blasse, G.; Grabmaier, B.C.; Ostertag, M. The Afterglow Mechanism of Chromium-Doped Gadolinium Gallium Garnet. *J. Alloys Compd.* **1993**, *200*, 17–18. [[CrossRef](#)]
34. Yamada, A.; Tanigawa, T.; Suyama, T.; Matsuno, T.; Kunitake, T. Red:Far-Red Light Ratio and Far-Red Light Integral Promote or Retard Growth and Flowering in *Eustoma Grandiflorum* (Raf.) Shinn. *Sci. Hortic.* **2009**, *120*, 101–106. [[CrossRef](#)]

35. Jia, Z.; Yuan, C.; Liu, Y.; Wang, X.J.; Sun, P.; Wang, L.; Jiang, H.; Jiang, J. Strategies to Approach High Performance in Cr³⁺-Doped Phosphors for High-Power NIR-LED Light Sources. *Light Sci. Appl.* **2020**, *9*, 2047–7538. [[CrossRef](#)]
36. He, S.; Zhang, L.; Wu, H.; Wu, H.; Pan, G.; Hao, Z.; Zhang, X.; Zhang, L.; Zhang, H.; Zhang, J. Efficient Super Broadband NIR Ca₂LuZr₂Al₃O₁₂:Cr³⁺,Yb³⁺ Garnet Phosphor for Pc-LED Light Source toward NIR Spectroscopy Applications. *Adv. Opt. Mater.* **2020**, *8*, 1901684. [[CrossRef](#)]
37. Ferrauto, G.; Carniato, F.; Di Gregorio, E.; Botta, M.; Tei, L. Photoacoustic Ratiometric Assessment of Mitoxantrone Release from Theranostic ICG-Conjugated Mesoporous Silica Nanoparticles. *Nanoscale* **2019**, *11*, 18031–18036. [[CrossRef](#)] [[PubMed](#)]
38. Cao, R.; Shi, Z.; Quan, G.; Chen, T.; Guo, S.; Hu, Z.; Liu, P. Preparation and Luminescence Properties of Li₂MgZrO₄:Mn⁴⁺ Red Phosphor for Plant Growth. *J. Lumin.* **2017**, *188*, 577–581. [[CrossRef](#)]
39. Inkraite, G.; Zabiliute-Karaliune, A.; Aglinskaite, J.; Vitta, P.; Kristinaityte, K.; Marsalka, A.; Skaudzius, R. Study of YAG:Ce and Polymer Composite Properties for Application in LED Devices. *Chempluschem* **2020**, *85*, 1504–1510. [[CrossRef](#)]
40. Chen, X.; Qin, H.; Zhang, Y.; Jiang, J.; Wu, Y.; Jiang, H. Effects of Ga Substitution for Al on the Fabrication and Optical Properties of Transparent Ce:GAGG-Based Ceramics. *J. Eur. Ceram. Soc.* **2017**, *37*, 4109–4114. [[CrossRef](#)]
41. Panatarani, C.; Faizal, F.; Florena, F.F.; Jumhur, D.; Made Joni, I. The Effects of Divalent and Trivalent Dopants on the Luminescence Properties of ZnO Fine Particle with Oxygen Vacancies. *Adv. Powder Technol.* **2020**, *31*, 2605–2612. [[CrossRef](#)]
42. Dickens, P.T.; Haven, D.T.; Friedrich, S.; Lynn, K.G. Scintillation Properties and Increased Vacancy Formation in Cerium and Calcium Co-Doped Yttrium Aluminum Garnet. *J. Cryst. Growth* **2019**, *507*, 16–22. [[CrossRef](#)]
43. Mao, M.; Zhou, T.; Zeng, H.; Wang, L.; Huang, F.; Tang, X.; Xie, R.J. Broadband Near-Infrared (NIR) Emission Realized by the Crystal-Field Engineering of Y_{3-x}Ca_xAl_{5-x}Si_xO₁₂:Cr³⁺ (x = 0–2.0) Garnet Phosphors. *J. Mater. Chem. C* **2020**, *8*, 1981–1988. [[CrossRef](#)]
44. Butkute, S.; Gaigalas, E.; Beganskiene, A.; Ivanauskas, F.; Ramanauskas, R.; Kareiva, A. Sol-Gel Combustion Synthesis of High-Quality Chromium-Doped Mixed-Metal Garnets Y₃Ga₅O₁₂ and Gd₃Sc₂Ga₃O₁₂. *J. Alloys Compd.* **2018**, *739*, 504–509. [[CrossRef](#)]
45. Chen, L.; Chen, X.; Liu, F.; Chen, H.; Wang, H.; Zhao, E.; Jiang, Y.; Chan, T.S.; Wang, C.H.; Zhang, W.; et al. Charge Deformation and Orbital Hybridization: Intrinsic Mechanisms on Tunable Chromaticity of Y₃Al₅O₁₂:Ce³⁺ Luminescence by Doping Gd³⁺ for Warm White LEDs. *Sci. Rep.* **2015**, *5*, 1–17. [[CrossRef](#)]
46. Yanagida, T.; Fujimoto, Y.; Yamaji, A.; Kawaguchi, N.; Kamada, K.; Totsuka, D.; Fukuda, K.; Yamanoi, K.; Nishi, R.; Kurosawa, S.; et al. Study of the Correlation of Scintillation Decay and Emission Wavelength. *Radiat. Meas.* **2013**, *55*, 99–102. [[CrossRef](#)]
47. Malysa, B.; Meijerink, A.; Jüstel, T. Temperature Dependent Luminescence Cr³⁺-Doped GdAl₃(BO₃)₄ and YAl₃(BO₃)₄. *J. Lumin.* **2016**, *171*, 246–253. [[CrossRef](#)]
48. Zhou, X.; Luo, X.; Wu, B.; Jiang, S.; Li, L.; Luo, X.; Pang, Y. The Broad Emission at 785 Nm in YAG:Ce³⁺, Cr³⁺ Phosphor. *Spectrochim. Acta Part A Mol. Biomol. Spectrosc.* **2018**, *190*, 76–80. [[CrossRef](#)]
49. Yanagida, T.; Fujimoto, Y.; Koshimizu, M.; Watanabe, K.; Sato, H.; Yagi, H.; Yanagitani, T. Positive Hysteresis of Ce-Doped GAGG Scintillator. In *Optical Materials*; Elsevier B.V.: Amsterdam, The Netherlands, 2014; Volume 36, pp. 2016–2019. [[CrossRef](#)]
50. Liu, W.-R.; Lin, C.C.; Chiu, Y.-C.; Yeh, Y.-T.; Jang, S.-M.; Liu, R.-S.; Cheng, B.-M. Versatile Phosphors BaY₂Si₃O₁₀:RE (RE = Ce³⁺, Tb³⁺, Eu³⁺) for Light-Emitting Diodes. *Opt. Express* **2009**, *17*, 18103. [[CrossRef](#)]
51. Spassky, D.; Kozlova, N.; Zabelina, E.; Kasimova, V.; Krutyak, N.; Ukhanova, A.; Morozov, V.A.; Morozov, A.V.; Buzanov, O.; Chernenko, K.; et al. Influence of the Sc Cation Substituent on the Structural Properties and Energy Transfer Processes in GAGG:Ce Crystals. *CrystEngComm* **2020**, *22*, 2621–2631. [[CrossRef](#)]
52. Katelnikovas, A.; Bettentrup, H.; Dutczak, D.; Kareiva, A.; Jüstel, T. On the Correlation between the Composition of Pr³⁺ Doped Garnet Type Materials and Their Photoluminescence Properties. *J. Lumin.* **2011**, *131*, 2754–2761. [[CrossRef](#)]
53. Zhou, D.; Tao, L.; Yu, Z.; Jiao, J.; Xu, W. Efficient Chromium Ion Passivated CsPbCl₃:Mn Perovskite Quantum Dots for Photon Energy Conversion in Perovskite Solar Cells. *J. Mater. Chem. C* **2020**, *8*, 12323–12329. [[CrossRef](#)]
54. Malysa, B.; Meijerink, A.; Jüstel, T. Temperature Dependent Cr³⁺ Photoluminescence in Garnets of the Type X₃Sc₂Ga₃O₁₂ (X = Lu, Y, Gd, La). *J. Lumin.* **2018**, *202*, 523–531. [[CrossRef](#)]
55. Dantelle, G.; Boulon, G.; Guyot, Y.; Testemale, D.; Guzik, M.; Kurosawa, S.; Kamada, K.; Yoshikawa, A. Research on Efficient Fast Scintillators: Evidence and X-Ray Absorption Near Edge Spectroscopy Characterization of Ce⁴⁺ in Ce³⁺, Mg²⁺-Co-Doped Gd₃Al₂Ga₃O₁₂ Garnet Crystal. *Phys. Status Solidi Basic Res.* **2020**, *257*, 1900510. [[CrossRef](#)]
56. Lucchini, M.T.; Baganov, O.; Auffray, E.; Bohacek, P.; Korjik, M.; Kozlov, D.; Nargelas, S.; Nikl, M.; Tikhomirov, S.; Tamulaitis, G.; et al. Measurement of Non-Equilibrium Carriers Dynamics in Ce-Doped YAG, LuAG and GAGG Crystals with and without Mg-Codoping. *J. Lumin.* **2018**, *194*, 1–7. [[CrossRef](#)]